Solar-Terrestrial Physics. 2025, vol. 11, iss. 4, pp. 39–48. DOI: 10.12737/stp-114202503. © 2025 V.A. Pilipenko, E.N. Fedorov, N.G. Mazur, E.N. Ermakova, A.V. Ryabov, A.S. Potapov, R.A. Marchuk, V.V. Kolobov, S.V. Anisimov, D.D. Pozdnyakova. Published by INFRA-M Academic Publishing House

DOI: 10.12737/stp-114202503

Received March 01, 2025
Accepted June 10, 2025

EXCITATION OF GLOBAL ARTIFICIAL Pc1 SIGNALS DURING FENICS-2024 EXPERIMENT: 2. MODELING

V.A. Pilipenko
Schmidt Institute of Physics of the Earth RAS, Moscow, Russia, pilipenko_va@mail.ru

E.N. Fedorov
Schmidt Institute of Physics of the Earth RAS, Moscow, Russia, enfedorov1@yandex.ru

N.G. Mazur
Schmidt Institute of Physics of the Earth RAS, Moscow, Russia, ngmazur@mail.ru

E.N. Ermakova
Institute of Radiophysics of Nizhny Novgorod University, Nizhny Novgorod, Russia, l.ermakova@nirfi.unn.ru

A.V. Ryabov
Institute of Radiophysics of Nizhny Novgorod University, Nizhny Novgorod, Russia, alexr@nirfi.unn.ru

A.S. Potapov
Institute of Solar-Terrestrial Physics SB RAS, Irkutsk, Russia, potapov@iszf.irk.ru

R.A. Marchuk
Institute of Solar-Terrestrial Physics SB RAS, Irkutsk, Russia, marchuk@iszf.irk.ru

V.V. Kolobov
Northern Energy Center KSC, Apatity, Russia, v.kolobov@ksc.ru

S.V. Anisimov
Borok Geophysical Observatory of Schmidt Institute of Physics of the Earth RAS, Borok, Russia, anisimov@borok.yar.ru

D.D. Pozdnyakova
Schmidt Institute of Physics of the Earth RAS, Moscow, Russia, d_pozdnyakova@live.ru

Abstract. During the active experiment FENICS-2024 on the Kola Peninsula using a decommissioned power transmission line as a horizontal radiating antenna, ultra-low-frequency signals of the 1–6 Hz range were recorded at magnetic stations located from ~1600 km to ~2100 km from the transmission line with normalized amplitudes from ~0.3 fT/A to ~0.8 fT/A. Observational results are compared with approximate analytical estimates of the magnetic field excited by the magnetic dipole. The calculations turned out to be in qualitative agreement with the observational results. To assess the possible response in the upper ionosphere, a numerical model of the ULF field in the atmosphere and ionosphere generated by the horizontal surface current was employed. The model is based on solving the system of Maxwell equations in the vertically inhomogeneous atmosphere and ionosphere. The fundamental feature of this model is that it correctly takes into account the contribution of ionospheric waveguide propagation. The observational results supported by numerical simulation have shown the potential of active experiments of the new type for signal generation for large-area magnetotelluric sounding and for modification of near-Earth plasma with artificial signals.

Keywords: ULF radiation, FENICS installation, active experiments, transmission lines, Pc1 pulsations, atmospheric waveguide, ionospheric waveguide.

INTRODUCTION: EXCITATION OF ARTIFICIAL VLF EMISSIONS

From July 25 to August 5, 2024, the FENICS-2024 experiment (Fennoscandian Electrical conductivity from soundings with the Natural and Controlled Sources) was conducted on the Kola Peninsula, using a temporarily decommissioned power transmission line (PTL) as a radiating antenna. At the first stage of the experiment on July 25–26, the submeridional transmission line Vykhodnoy—Olenegorsk L-400 was utilized as a radiating antenna (95.6 km long, distance between groundings at the power substations L=84 km). The generator connected to the PTL produced an alternating current in the line with an amplitude from ~150 A at low frequencies (~1 Hz) to ~40 A at high frequencies (~194 Hz). Artificial Pc1signals were detected at magnetic stations located ~1200–2100 km away from the transmission line [Pilipenko et al., 2025].

To theoretically interpret experimental results from the study of propagation of ULF-ELF signals along the Earth surface, relations from various approximate models are usually employed (e.g., [Makarov et al., 1993; Vaisleb, Sobchakov, 1979]). The analytical theory of excitation of normal waves by a horizontal magnetic dipole in a planar waveguide bounded by two planes has been worked out by Sobchakov et al. [2003]. In this case, one wall (the Earth surface) was assumed to be ideally conductive, and an impedance boundary condition independent of the horizontal wavenumber was set on the second wall. Permittivity between the walls was

supposed to be constant. Tereshchenko et al. [2018] have solved the problem of field excitation by a horizontal radiator of finite length in a medium of three layers with homogeneous and isotropic conductivities forming a planar waveguide. The ULF-ELF field of one normal wave in the horizontally inhomogeneous Earth—ionosphere waveguide was calculated using a two-dimensional telegraphic equation [Kirillov, 1996].

An important aspect of this problem is the question about the influence of the ionosphere on excitation and propagation of ULF-ELF signals. During experiments near the radiator (~80 km), the amplitude of recorded signals in the frequency range 10–100 Hz remained constant regardless of ionospheric conditions. However, at frequencies below 10 Hz, the average field level changed noticeably on some days (to ~10 %), which was attributed to the effect of ionospheric conditions [Tereshchenko et al., 2018]. It was also observed that received signals differed significantly from season to season during the day and at night, which was associated with the effect of the ionosphere [Tereshchenko et al., 2007]. During experiments with recording PTL signals having frequencies of the order of the first hertz at large distances (R=500–1000 km), analysis of amplitude-frequency and polarization characteristics of artificial signals also showed that ionospheric conditions affect their properties [Belyaev et al., 2002; Ermakova et al., 2005]. Nonetheless, in these works the ionosphere was modeled rather simplistically through corrections describing wave reflection from the conductive layer of the lower ionosphere. For the ULF band (1–10 Hz), it was taken into account that plasma distribution with height in the real ionosphere is sharply inhomogeneous, thereby forming an ionospheric Alfvén resonator (IAR) and a waveguide for fast magnetosonic (FMS) waves [Kirillov, Kopeikin, 2003; Tereshchenko, 2010]. Plasma conductivity is strongly anisotropic and gyrotropic, which leads to coupling of normal waves in the ionosphere. The model of ULF wave propagation from the surface horizontal magnetic dipole was further developed in [Ermakova et al., 2022] with due regard to the sphericity of the Earth—ionosphere waveguide. The surface impedance of the atmospheric waveguide upper wall was calculated by running an impedance matrix in the vertically inhomogeneous ionosphere from the ionosphere—magnetosphere boundary to the upper atmosphere, which yields a boundary condition on the upper wall of the waveguide. The calculations used the IRI model and took into account the inclination of the geomagnetic field. The calculations were performed for a distance of 1240 km corresponding to the FENICS experiment in 2001 [Ermakova et al., 2005]. The constructed model allowed us to describe polarization and frequency characteristics of signal at an observation point, to identify the manifestation of sub-IAR, and to assess horizontal irregularity effects.

To interpret the results of the FENICS-2024 experiment, we have employed a numerical model of the field in the atmosphere and ionosphere created by horizontal surface current, which most fully takes into account the vertically heterogeneous structure of the ionosphere. Previously, this model has successfully been used to calculate the response in the upper ionosphere to the operation of the ZEVS transmitter [Pilipenko et al., 2024b] and industrial PTLs [Fedorov et al., 2022; Fedorov et al., 2020, 2023]. In this paper, for the first stage of the FENICS-2024 experiment, we present the results of numerical modeling of the spatial structure of surface electromagnetic fields in the Pc1 range (1–10 Hz) excited by linear current. The results obtained by the numerical model are compared with analytical estimates of the fundamental normal wave field of the Earth—ionosphere waveguide excited by a magnetic dipole. The numerical model of finite source was employed to calculate the expected electromagnetic field in the ionosphere above the FENICS facility at satellite altitudes (800 km).

1. MODELING EXCITATION AND PROPAGATION OF ARTIFICIAL ULF SIGNALS

The PTL exploited in the experiment is located on a crystalline shield with an average conductivity $\sigma_g=10^{-4}$ S/m. For ULF frequencies, the wavelength in the atmosphere is longer or comparable to the characteristic scale of the irregularity of complex permittivity; therefore, propagation of the electromagnetic ULF field along the Earth surface and in the ionosphere cannot be described in terms of geometrical optics. It is necessary to find a solution of the complete system of Maxwell equations in the vertically inhomogeneous atmosphere and ionosphere. Simply put, the FENICS-2024 source is a horizontal wire with an oscillating current $J(t)=J_0\exp(-i\omega t)$, suspended at a height d above the ground and grounded at the ends. The length of the radiating line is assumed to be L=100 km. Current in PTL is closed by conduction currents in the earth's crust, concentrated in the skin layer $\delta_g=\sqrt{2}\left(\mu_0\sigma_g\omega\right)^{-1/2}$ thick. The task is to find the electromagnetic fields in the atmosphere and ionosphere, which are excited by such a current system. Let us use a Cartesian coordinate system with the Z-axis pointing vertically upward, with z=0 on the Earth surface; the X-axis directed along the current; and the Y-axis, across the current. The deviation from the geomagnetic field vertical in the PTL location area is small, so for simplicity we assume I=90°.

The wave field excited by a surface PTL-type source reaches a receiving point through several channels, as shown schematically in Figure 1:

- As a surface lateral wave propagating along the boundary between the conducting earth and the atmosphere. This wave can be described by analytical relations [Fock, 1972].
- As atmospheric normal waves between the earth and the lower edge of the ionosphere. In the atmospheric waveguide, all normal magnetic (H) and electric (E) waves fade away from the source at a distance about the height of the atmospheric waveguide, except for the E_0 wave (TH_0 mode). This mode does not have a cut-off frequency and can propagate over long distances at a speed comparable to the speed of light c.
- As FMS modes of the ionospheric waveguide in the F layer.

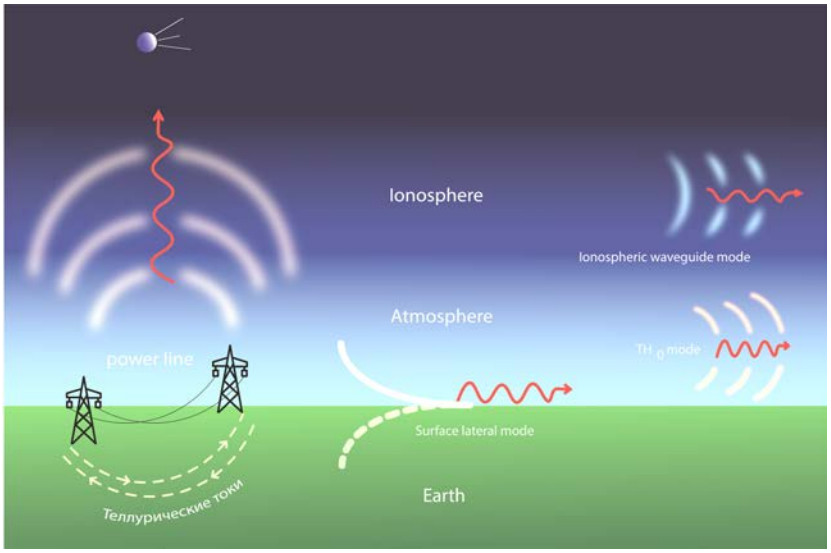

Figure 1. Qualitative illustration of wave modes excited by surface horizontal current

Let us examine a number of models, used to solve the problem, as they approach real conditions. First, rather crude analytical models are presented which describe the field in the immediate vicinity of a source and, vice versa, at a large distance from it, and ignore the ionospheric propagation channel. Then, we discuss the numerical model that better accounts for the actual structure of the atmosphere and ionosphere. We do not consider the models based on the telegraphic equation.

Infinite wire model for small distances

At small distances from PTL, the magnetic effect can be estimated by the formula for the horizontal magnetic field (B_y component) created by an infinite line with current J_0 at a height d above the Earth surface with finite conductivity σ_g [Boteler, Pirjola, 1998],

$$\frac{B_y}{J_0} = \frac{\mu_0}{2\pi}\left[\frac{d}{d^2+y^2} + \frac{d+2p}{(d+2p)^2+y^2}\right]. \qquad (1)$$

Here y is the distance from the projection of the current line on the plane z=0 to an observer; $\mu_0 = 4\pi\cdot 10^{-7}$ H/m is the magnetic constant; $p = (1+i)\delta_g/2 = (1+i)\left(2\omega\mu_0\sigma_g\right)^{-1/2}$ is the complex depth of imaginary current.

The results of calculation of the normalized field amplitude decrease with distance are presented in Figure 2 for the parameters corresponding to the experiment carried out on the Kola Peninsula. The calculation was made for three frequencies $f=(2\pi)^{-1}\omega$=1, 4, 10 Hz, for which $\delta_g = 50, 25, 16$ km respectively. At $y < \left(2d|p|\right)^{1/2}$ the magnetic field approximately coincides with the linear current field $B_y/J_0 \simeq (2\pi)^{-1}\mu_0 d/\left(d^2+y^2\right)$, and at $y \gg d$ it decreases as y^{-2} with a minimum at $y \approx \left(2d|p|\right)^{1/2}$. In the

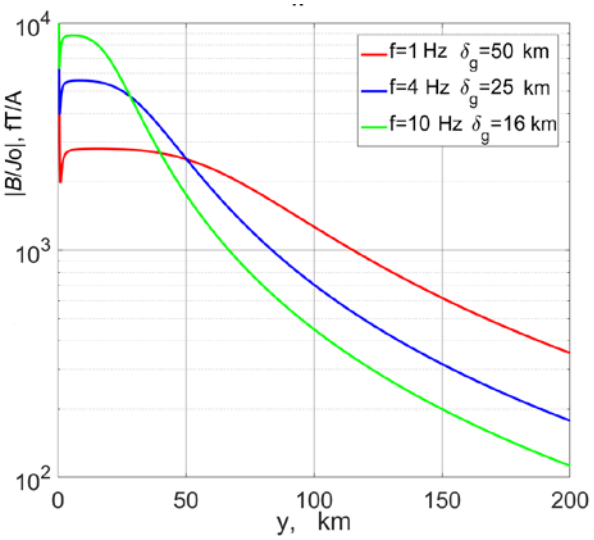

Figure 2. Calculation of a decrease in the normalized field amplitude for J_0=1 A with distance (0–200 km) for parameters corresponding to the experiment performed on the Kola Peninsula ($\sigma_g = 10^{-4}$ S/m). The calculation was carried out for three frequencies f=1, 4, 10 Hz from Formula (1). The corresponding values of the skin length are indicated in the legend

distance range $\left(2d|p|\right)^{1/2} < y < 2|p|$ the magnetic field changes little: $B_y/J_0 \approx (2\pi)^{-1}\mu_0/(4\pi p)$. With further increase in y at y>2 p, the field decreases as $B_y/J_0 \approx \mu_0\pi^{-1}p/y^2$.

Near the source at $y < \left(2d|p|\right)^{1/2}$ the magnetic field changes little with frequency. In the range of distances $\left(2d|p|\right)^{1/2} < y < 2|p|$, the ground magnetic response increases with frequency as $B \sim f^{1/2}$, and at $y > 2|p|$ it decreases as $B \sim f^{-1/2}$. However, the infinite source assumption makes it possible to use relation (1) only for distances $y<L$.

Dipole models for large distances from the source

To estimate signal amplitudes at large distances from the source $R \gg L$, we can assume that the current J_0 with a line length L and the current closing it in the earth's crust at a depth δ_g form a magnetic dipole with a moment $M = J_0 L \delta_g / \sqrt{2}$ [Polyakov, 2008]. When considering dipole radiation, it is natural to use cylindrical coordinates R, φ, z, where φ is the angle between the direction to the source and the extraneous current. The lower boundary of the ionosphere is at a height h.

Model 1. To estimate the magnitude of the field away from the radiator, a model of a planar waveguide between the conducting earth and the lower boundary of the ionosphere is considered, in which an impedance boundary condition is assumed [Sobchakov et al., 2003; Ryabov et al., 2020]. Taking into account the effect of the ionosphere in this model is reduced to introducing corrections describing wave reflection from an impedance layer with an impedance matrix independent of the incidence angle. The normalized modulus of the magnetic component of the TH_0 mode at intermediate distances ($h \ll R \ll k_0^{-1}$) is estimated from the relation [Ermakova et al., 2006]

$$\frac{B}{J_0} = \frac{i\mu_0 L\delta_g}{2^{3/2}\pi R^2 h}\left[1 - \frac{i\beta}{k_0 h}\right]^{-1}, \qquad (2)$$

where the coefficient $\beta = n_1^{-1} + n_2^{-1}$ (n_1, n_2 are the refractive indices of electromagnetic waves in the ionosphere), k_0=ω/c is the vacuum wavenumber. For rough estimates, the multiplier $\left[1 - i\beta/(k_0 h)\right]^{-1}$, which takes into account the effect of the upper gyrotropic wall, can be replaced by 1 since with characteristic ionospheric parameters $k_0 h \gg n_1^{-1}$ and $k_0 h \gg n_2^{-1}$, such that $\beta = n_1^{-1} + n_2^{-1} \ll k_0 h$. According to (2), the amplitude of the excited field decreases with distance from the source as $B(R) \propto R^{-2}$. In this case, the magnetic field decreases with increasing frequency as $B \sim f^{-1/2}$.

Model 2. In this model, permittivity in the atmosphere is not assumed to be constant in height because atmospheric conductivity increases rapidly with height. We seek for a solution in the form of the sum of normal waves of the atmospheric waveguide in view of the realistic dependence of permittivity $\varepsilon_a(z)$ on height. Since we are interested only in the contribution of atmospheric normal waves, we neglect the effect of ionospheric gyrotropy. We also ignore the Hall conductivity ($\sigma_H = 0$), but account for conductivity anisotropy (i.e. the transverse permittivity is not equal to the longitudinal one, $\varepsilon_\perp \neq \varepsilon_\parallel$). We look for the vertical component of the vector potential in the form of the sum of normal waves.

$$A_z(R, \varphi, z) = \sum_{j=0}^{\infty} d_j(R)\, y_1^{(j)}(z)\cos\varphi,$$

where $y_1^{(j)}(z)$ is the normal wave shape; the integral over the continuous spectrum is omitted. Let us set $\left(ik_0\varepsilon_\perp\right)^{-1}\partial_z y_1^{(j)}(z)\big|_{z=0} = 1$ and denote the normalization constant $N_{1j}^2 = \int\left[y_1^{(j)}(z)\right]^2/\varepsilon_\parallel(z)\,dz$ by N_{1j} For the distance dependence of the main normal wave amplitude E_0, we get

$$\frac{B}{J_0} = e^{-i\pi/4}\frac{i\mu_0 L\delta_g}{2^{3/2}\pi N_{10}^2 R^2}\left(\frac{k_0}{k_E^{(0)}}\right)^2, \qquad (3)$$

where $k_{TH}^{(0)}$ is the propagation constant in the atmosphere. In a realistic vertically inhomogeneous atmosphere, the propagation constant corresponds to a wave velocity ~100000–250000 km/s. Cartesian components of the wave field are found from formulas $B_x = -B\sin(2\varphi)$, $B_y = B\cos(2\varphi)$.

If we omit the multiplier $e^{-i\pi/4}$, neglect the height dependence of permittivity, assuming $\varepsilon_a \simeq 1$, and set the waveguide walls perfectly reflective, $k_E^{(0)} \simeq k_0$, $N_{10}^2 = h$, and Equation (3) transforms into (2) with β=0. In the case of height-varying permittivity, the height h is determined from $\varepsilon_\perp \approx \varepsilon_\parallel$ at $z<h$ and from $\varepsilon_\perp \ll \varepsilon_\parallel$ at $z>h$. Estimates from vertical atmospheric conductivity profiles give h≈50–60 km, and numerical calculations N_{10}^2 confirm the estimates.

Numerical model with a dipole source. The Fedorov—Mazur—Pilipenko (FMP) model is based on the numerical solution of the complete system of Maxwell equations in the vertically inhomogeneous atmosphere and ionosphere. The FMP numerical model with a realistic horizontally layered profile of the ionosphere, located in the vertical geomagnetic field, is based on the theory of wave excitation in the ionosphere by horizontal grounded current of finite length [Fedorov et al., 2022; Fedorov et al., 2023]. The vertical structure of ionospheric parameters is calculated using the IRI (International Reference Ionosphere) model for charged particles and the NRLMSISE-00 model for neutral particles. From the concentrations of electrons, ions, and neutrals and their temperatures obtained from these models, collision frequencies in ionospheric plasma and then components of the conductivity tensor as function of altitude z above ground and frequency are calculated. The IRI parameters are selected according to the conditions on July 25, 2024 at 23 UT and at the latitude of 69° N, where the radiating PTL is located.

Here we limit ourselves to a brief summary of the main points. Suppose the transverse components of the vector potential **A** satisfy the two-dimensional Coulomb gauge condition $\nabla_\perp \cdot \mathbf{A}_\perp = 0$. In this case, the solution of Maxwell equations with extraneous current in the form of a horizontal current dipole can be expressed through three potentials: the scalar potential Φ, the longitudinal component of the vector potential A_z, and the

auxiliary potential function Ψ. The transverse components of the vector potential satisfying the transverse Coulomb calibration can be represented as $\mathbf{A}_\perp = (ik_0)^{-1}\nabla\times\Psi\,\hat{\mathbf{z}}$. The potentials in use are slightly different from the usual ones since normalization of the electric field **e**=**E**/*c* is applied such that the vector **e** has the same dimension as the magnetic field **B**.

The introduced potentials excited in the anisotropic medium by the horizontal dipole can be found using the first-order Hankel transform with respect to the radial variable

$$\mathbf{K}_1\left[f(R)\right](k)=\int_0^\infty f(R)J_1(kR)RdR.$$

As a result, we arrive at a system of four ordinary differential equations in *z* depending on *k* as a parameter. For this system, a boundary value problem is formulated such that the natural boundary conditions include decay of disturbances at $z\to\pm\infty$. In addition, the matching condition is used at the source level $z=z_d$, where the solution experiences a jump proportional to the radiation current magnitude J_0.

To reduce the solution of this boundary value problem to the Cauchy problem, the admittance matrix recalculation method (or the boundary condition recalculation method) is adopted which facilitates the solution of equations in the presence of sharply increasing and decaying wave modes. Here, this method is applied not to the system of Maxwell equations, but to the system of potential equations. This system is divided into two 2D subsystems, and a 2D matrix **Y**(*z*) is introduced which transforms the unknowns of one of them, considered as a two-dimensional vector **v**(*z*), into a similar vector **u**(*z*) for the second subsystem: $\mathbf{u}(z)=\mathbf{Y}(z)\mathbf{v}(z)$. The matrix **Y**(*z*) satisfies the Riccati-type nonlinear differential equation $\partial_z\mathbf{Y}=\mathbf{S}-\mathbf{YTY}$, whose coefficients are defined by coefficients of the source system. In this case, the limiting values of the matrix **Y**(*z*) at $z\to\pm\infty$ are uniquely determined by combining solutions decaying at infinity. This allows us to find **Y**(*z*) from above and below the source level by numerically solving the corresponding Cauchy problems for the Riccati equation from +∞ or from –∞ to the source. In this case, different matrices $\mathbf{Y}(z_d+0)$ and $\mathbf{Y}(z_d-0)$ are obtained at the source level $z=z_d$. Comparing the jump of the matrix **Y**(*z*) with the matching condition at $z=z_d$ provides initial data to numerically solve the Cauchy problem for a system of equations defining potentials. Solving the Cauchy problem for this system numerically up and down from the source level, we find vertical profiles of the potentials and then all components of the electromagnetic field as function of *k*, φ, *z*. Finally, by applying the first-order inverse Hankel transform, we can obtain the spatial distribution of the field in cylindrical coordinates *R*, φ, z.

A feature of the numerical model for calculating the field on the Earth surface is an extremely slow decrease in the spatial spectrum with increasing radial wavenumber *k*, which complicates the numerical Hankel transform. To overcome such technical difficulties, it is necessary to preliminarily find the asymptotics of the spatial spectrum at $k\to\infty$ for each potential, assuming the permittivity of the atmosphere and ionosphere to be constant. The Hankel transform of these asymptotics is found in an analytical form, and the difference between the numerical and asymptotic spectra decreases at $k\to\infty$ quickly enough for the effective application of the numerical Hankel transform.

Numerical model of the field excited by finite length current. To identify an electromagnetic response near a source at ionospheric heights, the point dipole source theory described above becomes insufficient. The radiating line length ~100 km is comparable to the height of the lower edge of the ionosphere ~70 km above which the equipotentiality of geomagnetic field lines begins to manifest itself. Therefore, the disturbance caused by a finite-length line grounded at the ends is calculated by numerically summing up the fields from all the dipoles it is composed of.

2. MODELING RESULTS: PROPAGATION ALONG THE EARTH SURFACE

Let us examine the spatial structure of the magnetic component of artificial signals along the Earth surface. Figures 3 and 4 illustrate the dependence of the total amplitude of the horizontal component $|\mathbf{B}(R)|$ for distances to 2500 km at frequencies *f*=1 and 10 Hz with ground conductivity, characteristic of the Kola Peninsula, under experimental conditions. The field has been calculated for two directions: along (Figure 3, φ=0°) and across the current (Figure 4, φ=90°). The calculations were performed using approximate analytical models 1 and 2, and a numerical model. The contribution of a lateral wave, excluding the ionosphere and the atmospheric conductivity, is computed from Fock formulas [1972] for waves along a surface separating two homogeneous half-spaces. Note that at short distances $R\lesssim$300–500 km, the lateral wave makes the main contribution to the magnetic field.

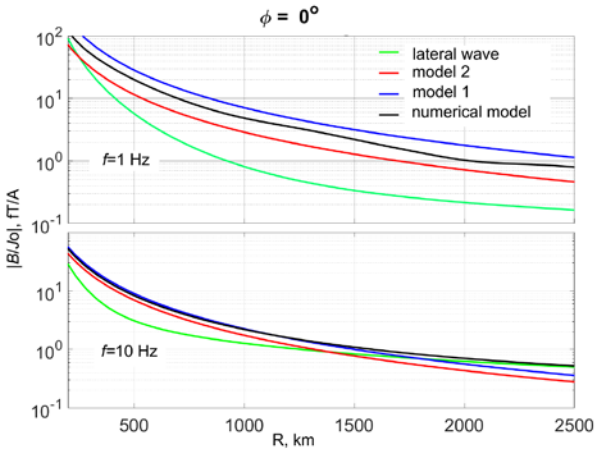

Figure 3. Decrease in the normalized magnetic field of signal with distance *R* at frequencies of 1 (*a*) and 10 Hz (*b*) for different models during propagation along the radiator current (φ =0°). The dipole and medium parameters are *L*=100 km, *h*=100 km, $\sigma_g=10^{-4}$S/m

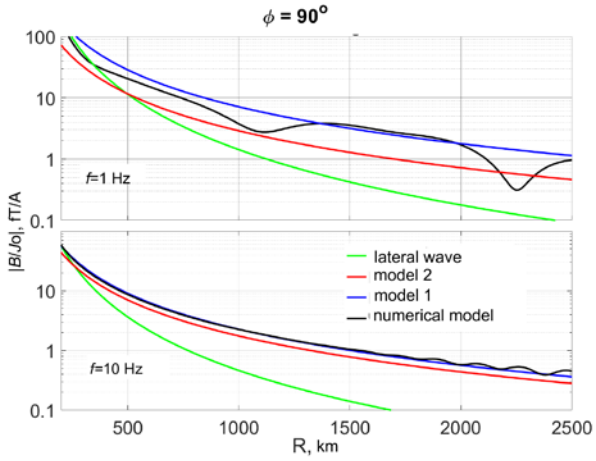

Figure 4. The same as in Figure 3, but for the direction across the extraneous current (φ=90°)

***Longitudinal propagation* (φ=0°).** Let us analyze the spatial structure of the field in the direction of the extraneous current at frequencies of 1 Hz (see Figure 3, top panel) and 10 Hz (see Figure 3, bottom panel). The amplitude of the excited electromagnetic field $|\mathbf{B}(R)|$ near the radiator (R<200 km) decreases sharply with distance, but decreases more slowly at long distances (R>300 km).

At 1 Hz, models 1 and 2 yield similar estimates, whereas model 1 shows an overestimate compared to model 2, although the difference is small (~2 times). At all distances $R \gtrsim 300$ km, the surface lateral wave makes a small contribution to the excited field. The results of the numerical model fall within the interval between the estimates made by models 1 and 2. At 10 Hz, models 1 and 2 give almost identical estimates, yet somewhat underestimated compared to the numerical model. Surprisingly, the contribution of the lateral surface wave becomes predominant from $R \approx 2000$ km. The artificial signal amplitude decreases with frequency, which is natural because the magnetic moment $M \sim f^{-1/2}$.

At distances of 1600 and 2100 km, the characteristic normalized amplitudes of the magnetic disturbance at 1 Hz are ~1.85 and 0.94 fT/A (see Figure 3, *a*). Thus, signal amplitudes at these two distances should differ about two times.

***Transverse propagation* (φ=90°).** Comparison between contributions of different channels to the amplitude of an artificial signal when propagating across extraneous current is shown for the frequencies of 1 Hz (see Figure 4, *a*) and 10 Hz (see Figure 4, *b*). At 1 Hz, model 1 yields an overestimate compared to model 2, but at 10 Hz models 1 and 2 give almost identical estimates. At all frequencies considered, at $R \gtrsim 500$ km the surface lateral wave makes a small contribution to $|\mathbf{B}(R)|$, so that at large distances the field is determined only by the sum of normal waves of the atmospheric and ionospheric waveguides.

At 1 Hz, the distance dependence of the excited field across the source current is oscillating, which is additional evidence for the existence of the ionospheric waveguide propagation channel. The amplitude of the total field calculated by the numerical model oscillates about the amplitude of the main atmospheric normal wave E_0. The characteristic spatial period of oscillations at 1 Hz is ~2400 km. The Alfvén velocity in the ionospheric waveguide is ~300–500 km/s, so the corresponding periods of spatial oscillations are less than 1000 km. The spatial period of several thousand kilometers is probably related to the interference of several normal waves of the ionospheric waveguide. At distances of 1600/2100 km across the source current, the characteristic normalized amplitudes of the magnetic disturbance at 1 Hz according to the numerical model are ~3.1/1.1 fT/A.

The R distance dependences of the total normalized magnetic field of the signal when propagating along the radiator current φ=0° and across the extraneous current φ=90° at the 1 Hz and 4 Hz frequencies for the numerical model are compared in Figure 5. On average, the amplitude at 1 Hz is higher than at 4 Hz. However, if the magnetic field amplitude $|\mathbf{B}(R)|$ at φ=0° decreases monotonously with distance, large-scale oscillations are superimposed at φ=90° against the background of the decrease. As a result, at R>1000 km the magnetic field amplitude at φ=90° is ~2 times higher/lower than the amplitude at φ=0° at the distances of interference maxima/minima. This difference is due to the fact that the excitation efficiency of the waveguide mode in the upper ionosphere across the current is higher than along the current. Since the position and depth of interference minima and maxima can vary markedly depending on frequency and parameters of the ionosphere, the ratio between signal amplitudes at the same distances in the longitudinal and transverse directions can vary several times.

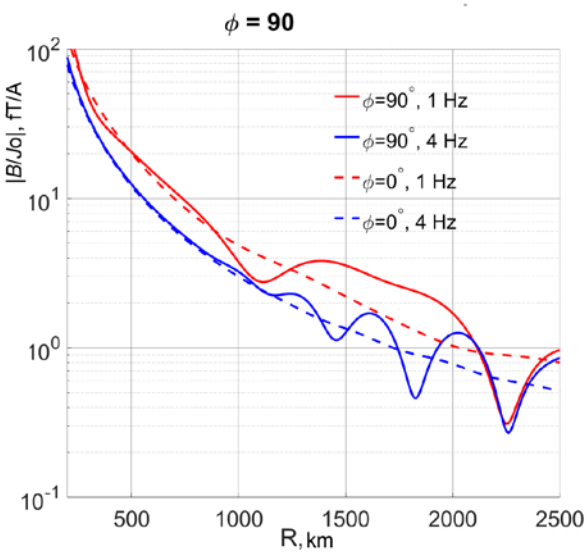

Figure 5. Comparison between R distance dependences of the normalized magnetic field of the signal when propagating along (φ=0°) and across (φ=90°) the radiator current at 1 Hz and 4 Hz frequencies for the numerical model

3. FIELD MODELING AT SATELLITE HEIGHTS

In a series of satellite observations supported by numerical modeling, PTL radiation at the fundamental frequency 50–60 Hz and its first harmonics was detected over industrialized areas [Pilipenko et al., 2021; Savelyeva et al., 2025]. The question arises: can hertz radiation emitted by PTL in the FENICS-2024 experiment be detected by a low-orbit satellite? If such an experiment could be carried out, it would be an excellent test of the idea of using PTLs as large-scale radiating antennas to excite artificial Pc1 pulsations [Pilipenko et al., 2024a]. For example, such an experiment could be performed with the Ionosphere-M mission spacecraft operating at an altitude of 800 km. However, calculating the passage of ULF radiation from horizontal mega-antennas through the ionosphere requires a realistic model of the ionosphere. Moreover, to describe the electromagnetic response at ionospheric heights, the dipole radiator theory becomes insufficient for a radiating line with a length comparable to the height of the lower edge of the ionosphere. In this case, it is necessary to have a model with a finite-length source.

To estimate which amplitude of artificial Pc1 signals could be expected at satellite altitudes in the vicinity of the source, we have carried out calculations with the FMP model for the same ionospheric conditions and PTL parameters (L=100 km), but for the altitude of the Ionosphere-M satellite (800 km). The total amplitude of the magnetic $|\mathbf{B}(R)|$ and electric $|\mathbf{E}(R)|$ components was calculated for f=1, 4, 10 Hz up to R=1000 km (Figure 6). At 1 Hz directly above the source (R=0 km), the normalized magnetic field amplitude is as high as $|\mathbf{B}/J_0|$~70 fT/A; and the electric field amplitude, $|\mathbf{E}/J_0|$~0.09 μV/mA. Thus, for typical currents J=150 A in the range 1–10 Hz during the FENICS-2024 experiment, the amplitudes of 1 Hz artificial Pc1 signals should be as high as $|\mathbf{B}| \sim 10$ pT and $|\mathbf{E}| \sim 13$ μV/m. A disturbance with such amplitudes would have been confidently recorded by the Ionosphere-M satellite equipment. If we assume that the threshold level of reliable detection of artificial Pc1 signals is $B^* \sim 1$ pT and $E^* \sim 1$ μV/m, a 1 Hz signal from a ground-based antenna with J_0=150 A should be detected at R^*~600 km in the magnetic component and at R^*~800 km in the electric component.

4. COMPARISON BETWEEN CALCULATIONS AND RESULTS OF GROUND OBSERVATIONS

During the first stage of the FENICS-2024 experiment at the stations S. Pustyn and Istok, located from the Vykhodnoy substation at a distance of ~1600 and ~2100 km, artificial radiation was reliably detected at 1–4 Hz frequencies with a normalized amplitude of 0.6 ±0.2 fT/A and 0.3±0.05 fT/A. When comparing the recorded signal amplitudes with calculations, the derived estimates should be reduced 100/84=1.2 times due to the difference between the model and actual line lengths L. Thus, the amplitudes predicted by the numerical model are ~1.5 fT/A at 1600 km (for the direction along the current) and ~0.9 fT/A at 2100 km (for the direction across the current). Halving in the field predicted by the numerical model between PUS and IST agrees well with

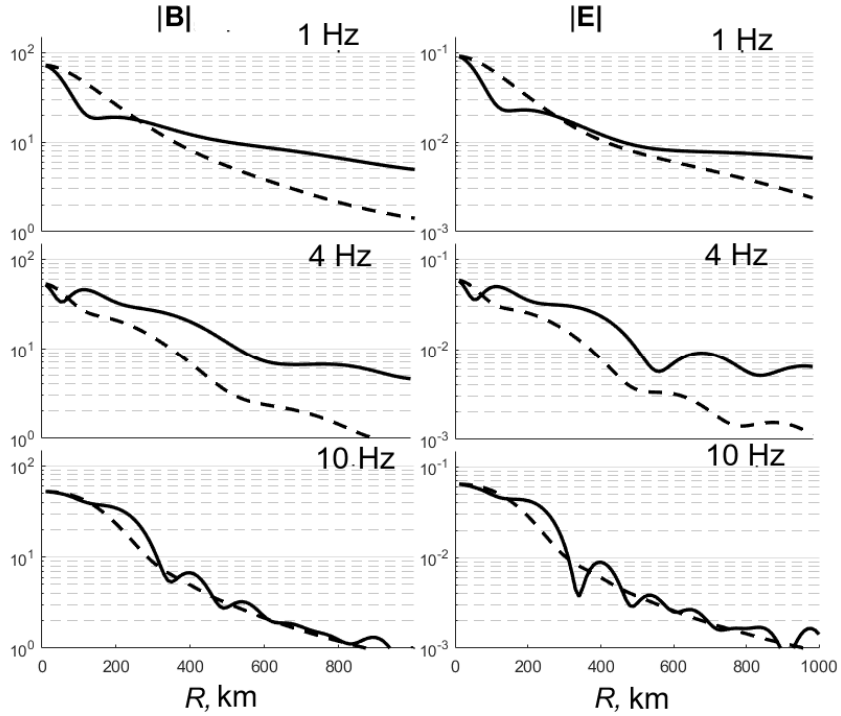

Figure 6. Calculations of the total amplitude of magnetic $|\mathbf{B}(R)|$ and electric $|\mathbf{E}(R)|$ components by the numerical model for the same ionospheric conditions and PTL parameters as in Figures 3–6, but for z=800 km. The calculations were performed for f=1, 4, 10 Hz up to R=1000 km

the measured ratio of signal amplitudes. The normalized signal amplitudes at remote stations turned out to be 2–3 times lower than those predicted by the numerical model.

Notice that the excited field is sensitive to the conductivity of the underlying Earth surface. Expressions (2) and (3) show that the magnetic field decreases with increasing conductivity approximately as $B \sim \sigma_g^{-1/2}$. The signal amplitude dependence calculated by the numerical FMP model is illustrated in Figure 7 for R=1000, 1610, 2100 km for f=1 Hz. For these distances, the amplitude decreases by about an order of magnitude with an increase in σ_g by two orders of magnitude from 10^{-5} to 10^{-3} S/m. According to the map of the model spatial distribution of the effective longitudinal conductivity of the earth's crust for the Russian Federation [Kozyreva et al., 2022], the conductivity on the Kola Peninsula ranges from 10^{-4} to 10^{-5} S/m. More accurate estimates of the expected amplitude of the disturbance at large distances require knowledge of the specific magnitude of crustal conductivity (or impedance) in the source and along the path.

It is impossible to reliably distinguish a clear frequency dependence of the recorded signal amplitude since signals only slightly exceed the noise level and the frequency range of received signals is narrow.

5. DISCUSSION

A basic feature of the numerical FMP model is that the contribution of ionospheric waveguide propagation to the excited field in the ULF band at large distances, which was previously taken into account in a simplified manner, is fully described in this model. Nonetheless, the model contains a number of simplifications: the vertical geomagnetic field, the horizontally homogeneous ionosphere and Earth surface conductivity, which affect the accuracy of derived estimates. Given the approximate nature of the model, a discrepancy of ~2 times

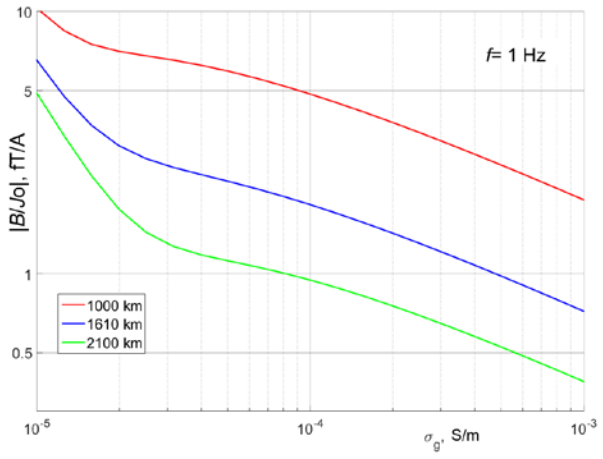

Figure 7. Signal amplitude calculated by the numerical model for three characteristic distances (indicated in the legend) for f=1 Hz as function of conductivity of the underlying surface σ_g [S/m]

seems quite acceptable. In principle, the developed algorithm based on numerical summation of elementary current sources allows us to calculate fields from PTLs of any configuration, not only from a current line of finite length.

Furthermore, although the current in the line was reliably measured, the effect of such a current source may be less than expected as the substations Vykhodnoy and Olenegorsk continued their work. Connections between the substations via active PTLs are therefore added to the ground circuit. This results in a slight decrease in the radiated magnetic moment due to the fact that not all reverse current flows in the ground, but part of the current flows back through active PTLs.

We have carried out a case study of the distances at which the planar-stratified medium model can still be used, examining the predominant TH_{10} mode in a spherical coordinate system through Legendre functions. Transition to the asymptotics of Legendre functions

$$\mathbf{E}, B \propto \frac{1}{\sqrt{\sin\vartheta}} \exp\left(i\nu\vartheta\right),$$

where ν is the wave number; ϑ — the spherical angle measuring the distance from the source shows that the flat-layered approximation is unsuitable for ϑ>1, i.e. at distances larger than the Earth radius R_E. Now let us estimate the effect of curvature on the angular wavenumber $\lambda=\nu(\nu-1)$. Consideration of the spectral problem in the first order according to perturbation theory for the normal mode gives the correction $\delta\nu_0/\nu_0=h/(2R_E)$. Finally, substituting $\nu_0 \approx k_0 R_E$, we find $\delta\nu_0 \sim k_0 h/2$. Thus, the higher the frequency and height of the upper boundary of the waveguide, the shorter the distances the 2D model is suitable for. We obtain that the correction $\delta\nu_0$ to the angular wavenumber can be neglected up to distances $x_* = 2R_E/(k_0 h)$. Thus, when estimating the angular wavenumber at f<100 Hz and h<100 km, the curvature can be ignored at $x < x_* \sim 10R_E$ and wavenumbers can be calculated without regard to sphericity.

The success of the FENICS-2024 experiment leads to the idea that PTL radiation can be utilized as a controlled source of ULF waves emitted into the upper ionosphere. According to numerical estimates, PTL ~100 km long with 150 A current produces hertz electromagnetic radiation in the upper ionosphere within a radius 600–800 km from the source, which can be detected by satellite equipment. Over the FENICS-2024 facility, we can expect excitation of artificial radiation with an amplitude up to a dozen picotesla, comparable to the amplitudes of natural Pc1 pulsations. The geomagnetic latitude of the FENICS facility on the Kola Peninsula corresponds to the center of Earth's outer radiation belt (L~6). Electrons of relativistic energies forming the radiation belt can resonantly scatter along pitch angles by hertz ion-cyclotron waves and precipitate into the atmosphere. In the future, a ground-based ULF radiator of the FENICS type can be employed to control the intensity level of the external radiation belt and as a tool for emptying the radiation belt [Pilipenko et al., 2024a].

Thus, the FENICS facility can be a much cheaper and more effective alternative to radio heating methods of exciting artificial Pc1 pulsations. The proposed methods of environmental probing with an ionospheric source are uncompetitive compared to ground-based sources such as PTLs grounded at the ends [Polyakov, 2008].

At the second stage of the FENICS-2024 experiment, the Vykhodnoy—Nickel (VKH-NIK) line L-403 205 km long and with the distance between groundings of the substations L=130 km was used as a radiating antenna. Calculations for this stage of the experiment and their comparison with observational data will be presented in the follow-up study.

CONCLUSION

The FENICS-2024 experiment has shown that horizontal radiators with 140–150 A currents can indeed be utilized as an artificial source of Pc1 waves. Artificial electromagnetic harmonic oscillations at specified frequencies can be used for operational magnetotelluric sounding over an area up to 2000 km. Decommissioned PTLs can be a much cheaper and more effective alternative to radio heating methods of exciting artificial Pc1 pulsations. The observations have demonstrated the potential of active experiments of the new type for modification of near-Earth plasma by ULF signals.

The work was carried out under Government assignments of the Ministry of Science and Higher Education of the Russian Federation by IPE RAS (FMWU-2025-0043, FMWU-2025-0049), SUNN NIRPhI (FSWR-2023-0038), and ISTP SB RAS (FWSE-2021-0005). Works on the use of PTLs as radiating antennas were undertaken by NERC KSC with the financial support from RSF (Grant No. 22-17-00208). Signals were recorded at the station Istok with the equipment of Shared Equipment Center “Angara” [http://ckp-rf.ru/ckp/3056/].

REFERENCES

Belyaev P.P., Polyakov S.V., Ermakova E.N., et al. First experiments on generation and receiving artificial ULF radiations (0.3–12 Hz) at a distance of 1500 km. *Izvestiya vuzov. Radiofizika* [Radiophysics and Quantum Electronics]. 2002, vol. 45, no. 2, pp. 156–162. (In Russian).

Boteler D.H., Pirjola R.J. The complex image method for calculating the magnetic and electric fields produced at the surface of the Earth by the auroral electrojet. *Geophysical Journal International*. 1998, vol. 132, pp. 31–40.

Ermakova E.N., Kotik D.S., Sobchakov L.A., Polyakov S.V., Vasil’yev A.V., Bösinger T. Experimental studies of the propagation of artificial electromagnetic signals in the range of 0.6–4.2 Hz. *Radiophysics and Quantum Electronics*. 2005, vol. 48, no. 9, pp. 788–799.

Ermakova E.N., Kotik D.S., Polyakov S.V., Bösinger T., Sobchakov L.A. A power line as a tunable ULF-wave radiator: Properties of artificial signal at distances of 200 to 1000 km. *J. Geophys. Res.* 2006, vol. 111, A04305. DOI: 10.1029/2005JA011420.

Ermakova E.N., Kotik D.S., Ryabov A.V. Characteristics of ULF magnetic fields in the 3D inhomogeneous Earth-ionosphere waveguide. *J. Geophys. Res.* 2022, vol. 127, e2021JA030025. DOI: 10.1029/2021JA030025.

Fedorov E.N., Mazur N.G., Pilipenko V.A., Vakhnina V.V. Modeling ELF electromagnetic field in the upper ionosphere from power transmission lines. *Radio Sci.* 2020, vol. 55, e2019RS006943. DOI: 10.1029/2019RS006943.

Fedorov E.N., Mazur N.G., Pilipenko V.A. Electromagnetic field in the upper ionosphere from horizontal ELF ground-based transmitter with finite length. *Radiophysics and Quantum Electronics*. 2022, vol. 65, pp. 635–648. DOI: 10.1007/s11141-023-10245-z.

Fedorov E.N., Mazur N.G., Pilipenko V.A., Vakhnina V.V. Generation of artificial ULF/ELF electromagnetic emission in the ionosphere by horizontal ground-based current system. *J. Geophys. Res*, 2023, vol. 128, e2023JA031590. DOI: 10.1029/2023JA031590.

Fock V.A. About calculation of AC electromagnetic field under the occurrence of plane boundary. In book: *Bursian V.P. Theory of Electromagnetic Waves Applied in Electric Prospecting*. Leningrad, Nedra, 1972, 368 p. (In Russian).

Kirillov V.V. Two-dimensional theory of propagation of electromagnetic waves of the ULF range in the Earth-ionosphere waveguide. *Radiophysics and Quantum Electronics*. 1996, vol. 39, no. 12, pp. 1103–1112.

Kirillov V.V. Kopeikin V.N. Formation of the resonant structure of the local inductance of the ionosphere in the range of 0.1–10 Hz. *Radiophysics and Quantum Electronics*. 2003, vol. 46, no. 1, pp. 1–12.

Kozyreva O.V., Pilipenko V.A., Dobrovolsky M.N., Zaitsev A.N., Marshalko E.E. Database of geomagnetic observations in Russian Arctic and its application for estimates of the space weather impact on technological systems. *Sol.-Terr. Phys*. 2022, vol. 8, iss. 1, pp. 39–50. DOI: 10.12737/stp-81202205.

Makarov G.I., Novikov V.V., Rybachek S.T. *Propagation of Radio Waves in the Earth-Ionosphere Waveguide Channel and in the Ionosphere*. Moscow: Nauka, 1993, 148 p. (In Russian).

Pilipenko V.A., Fedorov E.N., Mazur N.G., Klimov S.I. Electromagnetic pollution of near-Earth space by power line emission. *Sol.-Terr. Phys*. 2021, vol. 7, no. 3, pp. 105–113. DOI: 10.12737/stp-73202107.

Pilipenko V.A., Mazur N.G., Fedorov E.N., Shevtsov A.N. The possibility of experiments on generating artificial Ultra-Low-Frequency radiation in the ionosphere using the FENICS transmitter on the Kola peninsula. *Bulletin of the Russian Academy of Sciences: Physics*. 2024a, vol. 88, no. 3, pp. 331–337. DOI: 10.1134/S1062873823705482.

Pilipenko V., Zhao S., Savelieva N., Mazur N., Fedorov E., Ma Z. ELF emission in the topside ionosphere from the ZEVS transmitter detected by CSES satellite. *Adv. Space Res.* 2024b, vol. 74, no.10, pp. 4937–4947. DOI: 10.1016/j.asr.2024.07.074.

Pilipenko V.A., Ermakova E.N., Potapov A.S., et al. Excitation of global artificial Pc1 signals during FENICS-2024 experiment: 1. Observations. *Sol.-Terr. Phys*. 2025, vol. 11, no. 2, pp. 111–118. DOI: 10.12737/stp-112202511.

Polyakov S.V. Artificial ionospheric source of low-frequency electromagnetic fields in environmental sensing problems. *Radiophysics and Quantum Electronics*. 2008, vol. 51, no. 12, pp. 1026–1034.

Ryabov A.V., Pilipenko V.A., Ermakova E.N., et al. Registration and modeling of ULF-ELF signals at Staraya Pustyn station during FENICS-2019 experiment. *Nauka i tekhnologicheskie razrabotki* [Science and Technological Developments]. 2020, vol. 99, no. 2, pp. 16–35. (In Russian).

Savelyeva N.V., Pilipenko V.A., Mazur N.G., Fedorov E.N., Zhao S. Electromagnetic emissions from the ZEVS transmitter and northern power transmission line, registered on the CSES satellite. *Bull. Russian Academy of Sciences: Physics*. 2025, vol. 89, no. 5, pp. 742–750.

Sobchakov L.A., Astakhova N.L., Polyakov S.V. Excitation of electromagnetic waves in a flat waveguide with anisotropic upper wall. *Radiophysics and Quantum Electronics*. 2003, vol. 46, no. 12, pp. 1027–1037.

Tereshchenko E.D., Grigoriev V.F., Sidorenko A.E., Milichenko A.N., Molkov A.V., Sobchakov L.A., Vasiliev A.V. Influence of the ionosphere on electromagnetic waves from a ground-based emitter in the frequency range of 1–10 Hz. *Geomagnetism and Aeronomy*. 2007, vol. 47, no. 6, pp. 855–856.

Tereshchenko E.D., Ivanov N.V., Sidorenko A.E., Grigoriev V.F. Study of the propagation features in high latitudes of an artificial electromagnetic signal in the range of 0.1–10 Hz. *Geomagnetism Aeronomy*. 2010, vol. 50, no. 5, pp. 660–670.

Tereshchenko E.D., Tereshchenko P.E., Sidorenko A.E., Grigoriev V.F., Zhamaletdinov A.A. Influence of the ionosphere on the excitation of the electromagnetic field of the ELF range and lower frequencies in the near zone. *Journal of Technical Physics*. 2018, vol. 6, c. 907–913. DOI: 10.21883/JTF.2018.06.4602453.

Vaisleb Yu.V., Sobchakov L.A. Dipole near the plane boundary between two media. *Proc. "Aerials"*. 1979, vol. 27. Moscow, Svjaz, pp. 98–109. (In Russian).

URL: http://ckp-rf.ru/ckp/3056/ (accessed April 30, 2025).

Original Russian version: Pilipenko V.A., Fedorov E.N., Mazur N.G., Ermakova E.N., Ryabov A.V., Potapov A.S., Marchuk R.A., Kolobov V.V., Anisimov S.V., Pozdnyakova D.D., published in Solnechno-zemnaya fizika. 2025, vol. 11, no. 3, pp. 44–54. DOI: 10.12737/szf-114202503.

How to cite this article

Pilipenko V.A., Fedorov E.N., Mazur N.G., Ermakova E.N., Ryabov A.V., Potapov A.S., Marchuk R.A., Kolobov V.V., Anisimov S.V., Pozdnyakova D.D. Excitation of global artificial Pc1 signals during Fenics-2024 experiment: 2. Modeling. *Sol.-Terr. Phys*. 2025, vol. 11, iss. 4, pp. 39–48. DOI: 10.12737/stp-114202503.